Toxicology International
DOI: 10.18311/ti/2026/v33i3/54044
INFORMATICS JOURNALS
eISSN: 0976-5131 | Vol 33(3), 2026 | pp. 580-593

Therapeutic Effects of Silymarin on Sodium Arsenite-Induced Myocardial Toxicity in Wistar Rats

T. Gurukiran[1], Prashantkumar Waghe[1]*, M. Vijaykumar[1], Shrikant Kulkarni[2], Sanganagouda Patil[3], L. R. Ananthakrishna[4], Sabha Kounin[5], M. A. Baseer[1], D. Ganeshkumar[1], Anilkumar[1] and Shashikant[1]

[1]*Department of Veterinary Pharmacology and Toxicology, Karnataka Veterinary, Animal and Fisheries Sciences University, Veterinary College, Bidar - 585401, Karnataka, India*

[2]*Department of Veterinary Physiology and Biochemistry, Karnataka Veterinary, Animal and Fisheries Sciences University, Veterinary College, Bidar - 585401, Karnataka, India*

[3]*Department of Veterinary Physiology and Biochemistry, Karnataka Veterinary, Animal and Fisheries Sciences University, Veterinary College, Gadag - 582101, Karnataka, India*

[4]*Department of Veterinary Physiology and Biochemistry, Karnataka Veterinary, Animal and Fisheries Sciences University, Veterinary College, Vinobanagar, Shivamogga - 577204, Karnataka, India*

[5]*Institute of Animal Health and Veterinary Biologicals, Bellary Road, Next to Veterinary College, Bengaluru - 560024, Karnataka, India*

Abstract

Sodium (meta) Arsenite (SA), a widely encountered environmental metalloid, poses substantial cardiovascular hazards, especially in regions affected by contaminated drinking water. Silymarin (SM), a flavonolignan complex known for its antioxidant, anti-inflammatory, and cytoprotective actions, has gained attention for its potential to counter chemical-induced tissue damage. The present study investigated the cardioprotective role of SM against subacute SA-induced cardiovascular toxicity in male Wistar rats. Twenty-four rats were randomly assigned into four groups (n = 6) : Control, SM alone (100 mg/kg administered orally from day 14), SA alone (10 mg/kg in drinking water for 28 days), and SA + SM. Physiological parameters, body weight, feed and water intake were routinely monitored. On day 29, animals were euthanized and samples were collected for biochemical, and histopathological evaluations. SA exposure caused reduced water intake, feed intake, and poor body weight gain. Hematological analysis showed that SA reduced RBC count, hemoglobin, and platelets and increased CK-MB. SA markedly elevated superoxide anion, lipid peroxidation, depleted GSH, and reduced antioxidant enzyme activities. TNF-α levels and cardiac mRNA expression were significantly up-regulated. Histopathology of the heart revealed hemorrhage, myocardial necrosis, fiber disintegration, and inflammatory cell infiltration.Treatment with SM improved physiological, hematological, and biochemical (CK-MB) parameters, restored antioxidant status, suppressed TNF-α levels and mRNA expression, and enhanced myocardial structural integrity. SA induced marked cardiotoxicity characterized by oxidative stress, inflammation, hematological alterations, elevated CK-MB, and myocardial structural damage. SM significantly reversed these changes by restoring antioxidant status, reducing TNF-α–mediated inflammation, and improving cardiac tissue integrity, demonstrating a protective effect against established arsenic-induced cardiotoxicity. These findings indicate that SM exhibits significant therapeutic potential in ameliorating established SA-induced cardiotoxicity, warranting further mechanistic and clinical investigation.

Keywords: Antioxidant Defence, Silymarin, Sodium (meta) Arsenite, Wistar Rats

Article Received on: 12.12.2025 **Revised on:** 03.03.2026. **Accepted on:** 12.03.2026

*Author for correspondence

1. Introduction

Arsenic is a hazardous metalloid widely distributed in the environment, occurring in both organic and inorganic forms, with the inorganic variants being considerably more toxic[1]. Chronic exposure to arsenic, primarily through contaminated groundwater, is a serious public health issue in regions such as India, Bangladesh, and other parts of the world[2, 3]. Levels exceeding 0.01 ppm have been reported in tube well water in several Indian states, significantly increasing the risk for millions of residents[4, 5].

The cardiovascular system is notably susceptible to arsenic toxicity, with chronic exposure being closely linked to complications such as hypertension, ischaemic heart disease, peripheral vascular disease, and atherosclerosis[6]. The best-documented mechanism underlying arsenic-induced cardiovascular toxicity is oxidative stress, driven by an overproduction of reactive oxygen species or a decrease in antioxidant defence systems[7]. This imbalance results in damage at the DNA, protein, and lipid levels, often leading to cell death and tissue dysfunction in the heart[8]. Experimental findings consistently demonstrate that arsenic depletes cardiac antioxidant enzymes such as Superoxide Dismutase (SOD), catalaseand Glutathione Peroxidase (GPx), while elevating Lipid Peroxidation (LPO) and protein carbonyl accumulation[9, 10]. It may also upregulate pro-inflammatory cytokines, compounding oxidative and structural damage in the myocardium[11].

Silymarin (SM), a prominent flavonolignan complex from *Silybum marianum*, has demonstrated considerable potential due to its pronounced antioxidant, anti-inflammatory, and cardioprotective effects[12,13]. SM enhances endogenous antioxidant enzyme activities, scavenges reactive oxygen species, and downregulates the expression of inflammatory mediators such as TNF-α and IL-6[14, 15]. Its ability to stabilize biological membranes and inhibit oxidative stress-mediated injury underscores its therapeutic role in attenuating heavy metal-induced cardiac toxicity[16]. However, only limited studies have addressed the specific protective efficacy of SM against arsenic-induced heart injury, warranting further investigation[17].

2. Materials and Methods

2.1 Experimental Animals

Twenty-four male Wistar rats (weight: 100-150 g) were sourced from a CCSEA- authorized vendor Sri. Mahaveer Enterprises, Medchal - Malkajgiri, Telangana and maintained under standard management conditions in the Laboratory Animal House, Veterinary College, Bidar. The animals were provided with standard rat pellet feed (RAT NUTRIMIX 1020 FEED) and water *ad libitum*. The rats were housed 10 days before the actual start of the experiment to acclimate to the conditions. The protocol for the study was approved by the Institutional Animal Ethics Committee (IAEC), Veterinary College Bidar, 585 226, Karnataka (ApprovalNo. VCB/IAEC/VPT-49/2024-2025 dated 21/03/2025) to carry out the current study as per the guidelines ofthe Committee for Control and Supervision ofExperiments on Animals (CCSEA), New Delhi, India.

2.2 Chemicals and Reagents

Technical grade sodium (meta) arsenite ($NaAsO_2$, MW 129.91) and Silymarin were procured from Sigma-Aldrich, USA. All other analytical or molecular-grade chemicals were procured from certified suppliers.

2.3 Experimental Design

Animals were randomly divided into four groups, with six rats in each group. Group I served as the control and received only water. Group II received silymarin at a dose of 100 mg/kg orally for the last 14 days of the study. Group III was administered sodium meta-arsenite at 10 mg/kg orally for 28 consecutive days. Group IV received sodium meta-arsenite (10 mg/kg for 28 days) along with silymarin (100 mg/kg during the last 14 days) . All treatments were delivered through the oro-gastric route, maintaining a one-hour interval between administrations of different substances.

2.4 General Observation and Terminal Body Weight

During the experimental period, animals were monitored twice daily for clinical signs of toxicity (coat changes, posture, activity, diarrhoea, mortality), as well as weekly food intake, water intake and body weight.

2.5 Tissue Collection

Twenty-four hours after the last treatment, rats were anaesthetized with isoflurane. Blood was collected from the retro-orbital plexususing heparinized capillary tubesfor hematology and serum assays. For serum

biochemistry, blood was allowed to clot in plain tubes for 30 min at room temperature, followed by centrifugation at 1500 × g for 15 min; serum was stored at -20°C until analysis. After euthanasia, animals were positioned supine on a dissection tray, the abdominal area disinfected, and a midline incision made to expose visceral organs. Portions of heart tissue were snap-frozen at -20°C for oxidative stress assays, while the remaining tissue was fixed in 10% neutral-buffered formalin for histopathology.

Heart tissues were finely minced and homogenized in an ice-cold 50 mM potassium phosphate buffer (pH 7.4) using an IKA® homogenizer to obtain a 10% (w/v) homogenate. The samples were centrifuged at 10, 000 × g for 10 min at 4°C, and the resulting supernatant was aliquoted and stored at -20°C for estimation of Lipid Peroxidation (LPO), Reactive Oxygen Species (ROS), and antioxidant enzyme activities.

2.6 Measurement of Oxidative Stress Markers

2.6.1 Reactive Oxygen Species (ROS)

Superoxide anion ($O_2^{\bullet-}$) levels in heart tissue were quantified spectrophotometrically using the NBT (Nitroblue Tetrazolium) reduction method described by Wang *et al.*, [18]. Tissue homogenates were incubated with NBT at 37 °C, and the reaction was stopped with Hydrochloric Acid (HCl). Formazan formation was measured at 540 nm, and $O_2^{\bullet-}$ generation was expressed as pmol/min/mg protein.

2.6.2 Lipid Peroxidation (LPO)

Lipid Peroxidation (LPO) in heart tissue was assessed by quantifying Malondialdehyde (MDA) using the Thiobarbituric Acid Reactive Substances (TBARS) assay described by Paula *et al.*, [19]. Tissue homogenates were reacted with thiobarbituric acid and heated, and the resulting chromogen was measured at 535 nm. MDA levels were calculated using the extinction coefficient of the MDA–TBA complex and expressed as nmol MDA/g tissue.

2.6.3 Superoxide Dismutase (SOD) activity

Superoxide Dismutase (SOD) activity in heart tissue was determined spectrophotometrically at 570 nm using the method of Madesh and Balasubramanian[20]. The assay measured the inhibition of MTT reduction by the enzyme, and activity was expressed as units per milligram of protein, with one unit defined as the amount of SOD required to inhibit MTT reduction by 50%.

2.6.4 Catalase Activity

Catalase activity in heart tissue was estimated using the method of Aebi[21], by monitoring the decrease in absorbance of hydrogen peroxide (H_2O_2) at 240 nm. The rate of H_2O_2 decomposition was used to calculate enzyme activity, which was expressed as µmol H_2O_2 utilized per minute per milligram of protein.

2.6.5 Glutathione Peroxidase (GPx) Activity

Glutathione Peroxidase (GPx) activity in heart tissue was assessed using the method of Paglia and Valentine[22] by monitoring the decrease in absorbance of Nicotinamide Adenine Dinucleotide Phosphate (NADPH) at 340 nm. Enzyme activity was calculated from the rate of NADPH oxidation and expressed as µmol NADPH oxidized per minute per milligram of protein.

2.6.6 Glutathione Reductase (GR)

Glutathione Reductase (GR) activity in heart tissue was measured using the method of Goldberg and Spooner[23]. by monitoring the decrease in NADPH absorbance at 340 nm. Activity was calculated from the rate of NADPH oxidation and expressed as µmol NADPH oxidized per minute per milligram of protein.

2.6.7 Reduced Glutathione (GSH)

Glutathione Reductase (GSH) content in heart tissues was determined using the 5, 5′-Dithiobis(2-nitrobenzoic acid) (DTNB) method of Sedlak and Lindsay[24]. Tissue homogenates were deproteinized, reacted with DTNB, and absorbance was read at 412 nm. GSH levels were calculated using the extinction coefficient and expressed as mmol GSH per gram of wet tissue.

2.7 Biochemical Parameter

Serum Creatine-Kinase Myocardial Band (CK-MB) levels were measured using a commercially available enzymatic assay kit according to the manufacturer's instructions.

2.8 Inflammatory Cytokine Assay (TNF-α)

Tumour Necrosis Factor-alpha (TNF-α) levels in the heart were quantified using rat-specific ELISA kits

(KRISHGEN Biosystems; Cat. No. KB3145) based on the sandwich ELISA principle. Approximately 50-100 mg of tissue was homogenized in 1 ml cold Phosphate-Buffered Saline (PBS) and centrifuged at 10, 000 rpm for 15 min at 4°C. The assay was performed according to the manufacturer's instructions, and TNF-α concentrations were expressed as pg/mL.

2.9 Real-Time PCR Analysis of TNF-α Gene Expression

2.9.1 RNA Isolation and Quantification

Total RNA was isolated from approximately 50 mg of heart tissue preserved in RNAlater® using TRIzol™ reagent (Invitrogen, Thermo Fisher Scientific, USA) following the manufacturer's instructions. Tissue was homogenized in 1 mL TRIzol, phase-separated with chloroform, and centrifuged at 12, 000 × g for 15 min. The aqueous phase was precipitated with isopropanol, and the RNA pellet was washed with 70% ethanol, air-dried, and dissolved in nuclease-free water. RNA purity and concentration were assessed by NanoDrop® (A260/A280: 1.8–2.0), and 5 µg of high-quality RNA was used for cDNA synthesis.

2.9.2 cDNA Synthesis

First-strand cDNA was synthesized from 5 µg of total RNA using the RevertAid® First Strand cDNA Synthesis Kit (Thermo Fisher Scientific, USA) with random hexamer primers, following the manufacturer's recommended protocol.

2.9.3 Primer Sequences

Gene-specific primers for TNF-α (target gene) and β-actin (housekeeping gene) were designed and obtained from Bionova Supplies (Bangalore, India) .

β-actin:Forwardprimer:5'-CCTAGACTTCGAGCAAGAGATG-3';

Reverse primer: 5'-CAGGATTCCATACCCAGGAAG-3'

TNF-α:Forwardprimer:5'-AAATGGGCTCCCTCTCATCAGTTC-3';

Reverse primer: 5'-TCTGCTTGGTGGTTTGCTACGAC-3'

2.9.4 Quantitative Real-Time PCR (qRT-PCR)

Quantitative real-time PCR was performed using SsoFast™ EvaGreen®/SYBR Green Supermix (Bio-Rad) in a 20 µl reaction containing 10 µl master mix, 1 µl each of forward and reverse primers (10 pmol), 1 µl cDNA, and nuclease-free water. Reactions were run in duplicate on a Bio-Rad T100™ system under the following cycling conditions: initial denaturation at 95°C for 5 min, followed by 40 cycles of denaturation at 95°C for 15s, annealing at 62°C for 30s Safarpour *et al.*, [25] and extension at 72°C for 30s. A melt-curve analysis (65-95°C) confirmed amplification specificity. CT values were generated using Bio-Rad CFX Manager software, and relative TNF-α expression was calculated using the $2^{-\Delta\Delta CT}$ method Livak and Schmittgen[26] normalizing against β-actin to account for sample-to-sample variability.

2.10 Histopathology

Heart tissues from all groups were fixed in 10% neutral buffered formalin, washed, and dehydrated through graded alcohols before clearing in xylene and embedding in paraffin. Sections of ~5 µm thickness were prepared using a rotary microtome and mounted on glass slides. Standard hematoxylin and eosin (H and E) staining was performed, followed by dehydration, xylene clearing, and mounting with DPX. Slides were examined under a light microscope, and histopathological alterations were recorded using established morphological criteria.

2.11 Statistical Analysis

All data were expressed as mean ± SE. Statistical analysis of data was performed using IBM SPSS Statistics 25. Data were analyzed by one-way ANOVA followed by Duncan's multiple comparison post-hoc test. A mean value of (p<0.05) was considered statistically significant.

3. Results

3.1 Assessment of Water Intake, Feed Intake, and Body Weight

Mean ± SE values of weekly water intake (mL) for the CON, SM, SA, and SA + SM groups are presented in Table 1. Water intake remained comparable among all groups during week 0 and week 1, with no significant differences. A noticeable decline in water intake was observed in the SA group beginning from week 2, which became more pronounced in weeks 3 and 4, showing a statistically significant (p< 0.05) reduction compared

Table 1. Effects of silymarin on weekly water intake (mL), feed intake (gm) and body weight (gm) in sodium arsenite-exposed rats.

Week	Water intake (mL)				Feed intake (gm)				Body weight (gm)			
	CON	SM	SA	SA +SM	CON	SM	SA	SA +SM	CON	SM	SA	SA +SM
0	25.38 ± 0.32^{a}	25.56 ± 0.76^{a}	23.96 ± 0.77^{a}	24.33 ± 0.60^{a}	15.06 ± 0.13^{a}	15.02 ± 0.08^{a}	15.01 ± 0.19^{a}	15.14 ± 0.11^{a}	81.33 ± 2.19^{a}	86.67 ± 3.61^{a}	84.50 ± 2.57^{a}	84.67 ± 3.07^{a}
1	26.28 ± 0.47^{a}	26.08 ± 0.95^{a}	25.83 ± 0.52^{a}	25.22 ± 0.66^{a}	15.82 ± 0.21^{a}	15.49 ± 0.17^{a}	15.20 ± 0.32^{a}	15.12 ± 0.18^{a}	100.33 ± 2.14^{a}	100.33 ± 1.28^{a}	100.00 ± 1.15^{a}	98.83 ± 1.87^{a}
2	27.23 ± 0.36^{a}	27.68 ± 0.34^{a}	25.47 ± 0.36^{b}	25.05 ± 0.68^{b}	16.48 ± 0.08^{a}	16.33 ± 0.25^{a}	15.58 ± 0.19^{b}	15.59 ± 0.11^{b}	131.83 ± 2.70^{a}	131.50 ± 1.52^{a}	129.17 ± 1.54^{a}	129.33 ± 2.74^{a}
3	28.86 ± 0.51^{a}	27.74 ± 0.52^{a}	19.41 ± 0.67^{b}	22.72 ± 0.49^{c}	17.38 ± 0.13^{a}	17.43 ± 0.09^{a}	14.86 ± 0.25^{b}	14.85 ± 0.13^{b}	155.17 ± 3.97^{ab}	159.33 ± 2.47^{a}	141.83 ± 2.85^{c}	149.83 ± 1.70^{bc}
4	29.73 ± 0.42^{a}	27.02 ± 0.42^{a}	18.58 ± 0.70^{b}	24.03 ± 0.68^{c}	17.86 ± 0.02^{a}	17.81 ± 0.05^{a}	12.89 ± 0.15^{b}	14.88 ± 0.06^{c}	174.17 ± 4.90^{a}	180.00 ± 4.16^{a}	149.67 ± 2.60^{c}	161.83 ± 1.28^{b}

Values in the same rows (mean ± SE; n=6) bearing different superscripts vary significantly (p <0.05) in Duncan's multiple comparison post-hoc test. [CON: Control, SA: Sodium arsenite, SM: Silymarin, SA+ SM: Sodium arsenite + Silymarin].

to the control. In the SA + SM group, water intake also decreased from week 2; however, the reduction was less severe than in the SA group. A gradual improvement was observed in weeks 3 and 4, with values tending closer toward the control group. The SM group maintained weekly water intake similar to that of the control throughout the 4-week study period, with no significant variations.

Mean ± SE values of weekly feed intake (g) for the CON, SM, SA, and SA + SM groups are shown in Table 1. Feed intake was comparable among all groups during week 0 and week 1. From week 2 onward, the SA group showed a statistically significant (p <0.05) decline in feed intake, which continued through weeks 3 and 4, with the lowest values recorded in week 4. A similar reduction in feed intake was observed in the SA + SM group starting from week 2; however, the decline was less severe than in the SA group. Slight improvement was evident by week 4, indicating a protective trend toward control levels. Feed intake in the SM group remained comparable to that of the control group during all four weeks, with no significant deviations from normal consumption.

Table 1 shows the effects of SM on body weight (gm) in SA-exposed rats. Initial weights were similar across all groups (CON: 81.33 ± 2.19; SM: 86.67 ± 3.61; SA: 84.50 ± 2.57; SA + SM: 84.67 ± 3.07). Throughout the study, control and SM-treated rats showed steady weight gain, reaching 174.17 ± 4.90 and 180.00 ± 4.16 by week fourth, respectively. In SA-exposed rats, body weight increased during the first two weeks in a manner comparable to controls; however, from the third week onward, weight gain was markedly attenuated, with values remaining significantly lower than those of the control and SM groups 141.83 ± 2.85 at third week and 149.67 ± 2.60 at fourth week. SM administration in SA-exposed rats improved weight to 149.83 ± 1.70 at third week and 161.83 ± 1.28 at fourth week, indicating recovery toward normal growth.

3.2 Haematology

Table 2 summarizes the effects of SA and SM on hematological indices in rats. SA exposure produced a significant (p< 0.05) reduction in Red Blood Cells (RBC) count (6.68 ± 0.35 ×10^6/µL) compared to control (8.21 ± 0.24), whereas SM alone (8.16 ± 0.16) remained comparable to baseline administration of SM with SA (7.88 ± 0.28) markedly improved RBC values toward normal. White Blood Cells (WBC) counts did not differ significantly among groups, although SA caused a numerical decline (11.50 ± 0.92 ×10^3/µL) relative to control (16.13 ± 2.85) SM alone (15.70 ± 3.61 ×10^3/µL) maintained normal values, and SA+SM (12.83 ± 0.66 ×10^3/µL) partially restored WBC levels. Haemoglobin (Hb) concentration significantly decreased in SA-treated rats (14.68 ± 0.58 g/dL) compared to control (16.33 ± 0.37), while SM alone (16.80 ± 0.53) showed no deviation. SA+SM (15.78 ± 0.51) produced a moderate rise compared to SA. Packed Cell Volume (PCV) values were statistically unchanged among groups, though slightly reduced in SA (43.75 ± 1.62) compared to control (47.93 ± 1.33). SM alone (47.80 ± 1.12) remained normal, and SA+SM (46.23 ± 1.16) showed partial recovery. Mean Corpuscular Volume (MCV) values remained unaltered overall, with mild reduction seen in SA (58.95 ± 1.17 fL) and SA+SM (59.10 ± 0.86 fL) relative to control (61.45 ± 0.97 fL) . Mean Corpuscular Hemoglobin (MCH) showed a significant reduction (p < 0.05) in the SA group (19.65 ± 0.46) compared to control (21.03 ± 0.29) . SM alone (20.85 ± 0.52 pg) remained near baseline, while SA+SM (19.88 ± 0.23) showed slight improvement. Mean Corpuscular Hemoglobin Concentration (MCHC) was significantly decreased in SA (32.65 ± 0.54) versus control (34.28 ± 0.55). SM alone (34.95 ± 0.37) matched control values, and SA+SM (33.85 ± 0.37) provided moderate recovery. Platelet count was significantly reduced by SA (555.25 ± 24.90) compared to control (709.50 ± 42.80) . SM alone (633.50 ± 61.26) remained close to control, and SA+SM (586.75 ± 21.68) showed slight improvement.

3.3 Assessment of Oxidative Stress Biomarkers

3.3.1 Superoxide Radical ($O_2^{\bullet-}$) Generation

The effects of SM on $O_2^{\bullet-}$generation in the heart of SA-exposed rats were presented in Figure 1a, measured as reduced NBT levels (pmol/min/mg protein) . The control group recorded 86.83 ± 6.82, and SM alone (90.65 ± 5.64) maintained similar levels. In SA-exposed rats, $O_2^{\bullet-}$ levels were significantly (p< 0.05) increased to 200.89 ± 6.46, which was reduced to 167.80 ± 5.37 by SM, showing a moderate recovery.

3.3.2 Lipid Peroxidation (LPO) Level

Figure 1billustrated the LPO level in the heart(nmol MDA/g tissue) of SA-exposed rats. The control group exhibited 74.76 ± 6.41, while SM treatment alone (69.46 ± 8.17) did not produce significant changes. Exposure to SAmarkedly ($p < 0.05$) increased LPO levels to 138.73 ± 6.20, and subsequent SM administration significantly ($p < 0.05$) lowered them to 104.39 ± 4.02, indicating attenuation of SA-induced LPO in cardiac tissue.

3.3.3 Superoxide Dismutase (SOD) Activity

The cardiac SOD activity (units/mg protein) in SA-exposed rats was shown in Figure 2a. The control group recorded SOD activity of (0.61 ± 0.07) and SM treatment alone (0.60 ± 0.04) showed similar levels, indicating no significant change. SA exposure significantly ($p < 0.05$) reduced SOD activity to 0.35 ± 0.05. Administration of SM in SA-exposed rats increased SOD activity to 0.43 ± 0.01, which was significantly higher than the SA group, demonstrating a partial restoration of SOD activity in the heart.

3.3.4 Catalase Activity

The impact of SM on cardiac catalase activity (mmol H_2O_2 utilized/min/mg protein) in SA-exposed rats was presented in Figure 2b. The control group exhibited catalase activity of 99.08 ± 7.64, and SM alone (98.67 ± 7.10) maintained similar levels. Catalase activity decreased significantly ($p< 0.05$) to 71.62 ± 4.05 following SA exposure, and administration of SM partially restored it to 89.41 ± 4.44, reflecting significant recovery toward normal levels.

3.3.5 Glutathione Peroxidase (GPx) Activity

Effect of SM on cardiac GPx activity (µmol NADPH oxidized/min/mg protein) in SA-exposed rats was depicted in Figure 2c. GPx activity in the control group was 10.35 ± 1.31, and SM alone (10.47 ± 1.03) maintained activity at a level comparable to the control. SA significantly ($p < 0.05$) impaired GPx activity (4.77 ± 0.46), which was ameliorated by SM treatment to 7.70 ± 0.40 in the SA-exposed rats.

3.3.6 Glutathione Reductase (GR) Activity

The effects of SM on GR activity (µmol NADPH oxidized/min/mg protein) in the heart of SA-exposed rats were presented in Figure 2d. The control group recorded 2247.96 ± 87.84. which remained unchanged with SM alone (2276.01 ± 64.24) . SA significantly ($p< 0.05$) decreased GR activity to 1483.60 ± 76.27, and this effect was reversed with SM to 1908.24 ± 33.37, approaching control values.

3.3.7 Estimation of Reduced Glutathione (GSH)

The effect of SM on GSH content (mmol GSH/g tissue) in the heart of SA-exposed rats is depicted in Figure 2e. In the control group, GSH levels were 0.29 ± 0.01, and administration of SM alone (0.30 ± 0.01) did not produce significant changes. SA exposure caused a significant ($p < 0.05$) reduction to 0.25 ± 0.01. However, treatment with SM in SA-exposed rats significantly improved GSH levels to 0.28 ± 0.01, restoring them near control values.

Table 2. Effects of silymarin on haematological parameters in sodium arsenite-exposed rats.

Parameters	CON	SM	SA	SA + SM
RBC (10^6/µL)	8.21 ±0.24^a	8.16±0.16^a	6.68±0.35^b	7.88±0.28^a
WBC (10^3/µL)	16.13 ±2.85^a	15.70**±3.61**^{a}	11.50±0.92^a	12.83±0.66^a
Hb (g/dL)	16.33 ±0.37^a	16.80±0.53^a	14.68±0.58^b	15.78±0.51^{ab}
PCV (%)	47.93 ±1.33^a	47.80±1.12^a	43.75±1.62^a	46.23±1.16^a
MCV (*f*L)	61.45 ±0.97^a	60.30±0.90^a	58.95±1.17^a	59.10±0.86^a
MCH (pg)	21.03 ±0.29^a	20.85±0.52^{ab}	19.65±0.46^b	19.88±0.23^{ab}
MCHC (g/dL)	34.28 ±0.55^a	34.95±0.37^a	32.65±0.54^b	33.85±0.37^{ab}
PLT (10^3/µL)	709.50±42.80^a	633.50±61.26^{ab}	555.25±24.90^b	586.75±21.68^{ab}

Values in the same rows (mean ± SE; n=6) bearing different superscripts vary significantly ($p <0.05$) in Duncan's multiple comparison post-hoc test. [CON: Control, SA: Sodium arsenite, SM: Silymarin, SA+ SM: Sodium arsenite + Silymarin].

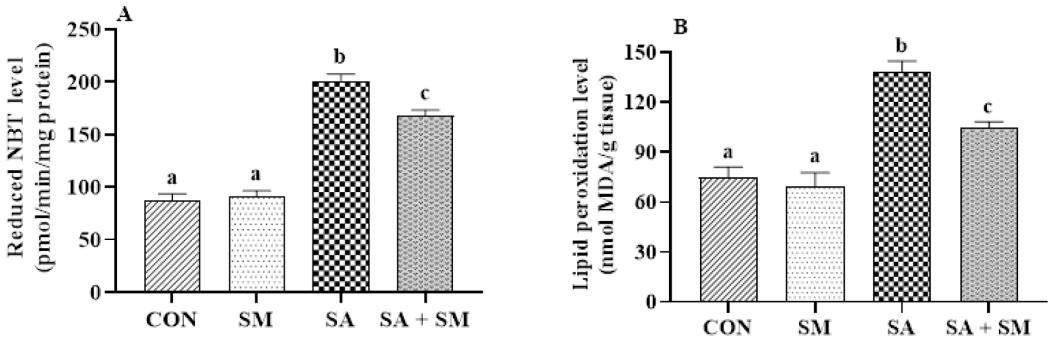


Figure 1: Effects of Silymarin on **(A)** superoxide anion radical ($O_2^{\bullet-}$) generation in terms of reduced nitroblue tetrazolium (NBT) content (pmol/min/mg protein) and **(B)** lipid peroxidation (LPO) levels (nmol MDA/g tissue) in the heart of sodium arsenite-exposed rats. Each bars represents mean ± SE (n=6) bearing different superscripts vary significantly (p <0.05) in Duncan's multiple comparison post-hoc test. [CON: Control, SA: Sodium arsenite, SM: Silymarin, SA+ SM: Sodium arsenite + Silymarin].

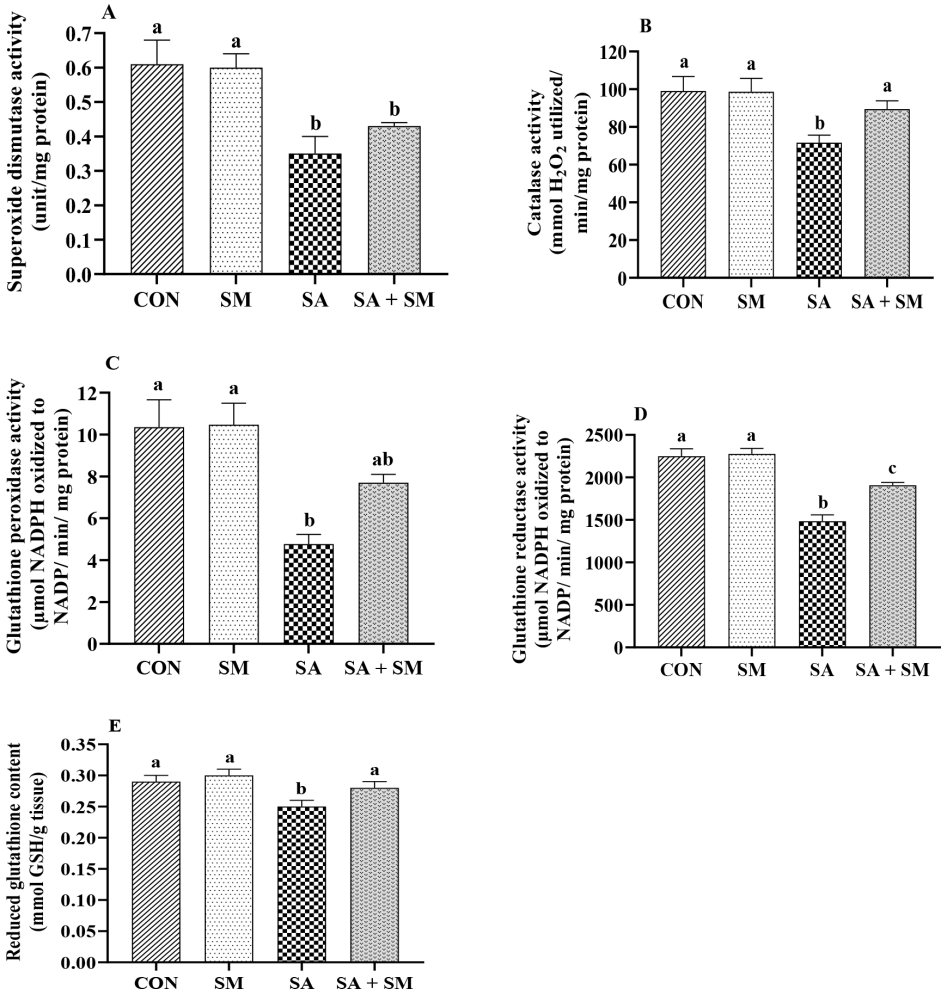


Figure 2: Effects of silymarin on **(A)** superoxide dismutase (SOD) activity (units/mg protein) **(B)** Catalase activity (mmol H_2O_2 utilized/min/mg protein) **(C)** Glutathione peroxidase (GPx) activity (µmol NADPH oxidized to NADP/ min/mg protein) **(D)** Glutathione reductase (GR) activity (µmol NADPH oxidized to NADP/ min/mg protein) **(E)** reduced glutathione (GSH) content (mmol GSH/g tissue) in the heart of sodium arsenite-exposed rats. Each bars represents mean ± SE (n=6) bearing different superscripts vary significantly (p <0.05) in Duncan's multiple comparison post-hoc test. [CON: Control, SA: Sodium arsenite, SM: Silymarin, SA+ SM: Sodium arsenite + Silymarin].

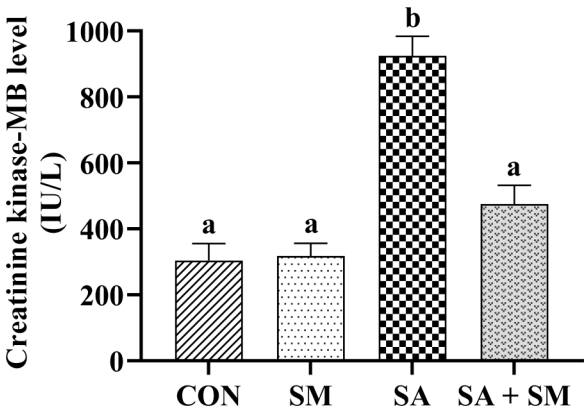


Figure 3: Effects of silymarin on creatine kinase-myocardial bond (CK-MB) level (IU/L) in sodium arsenite-exposed rats. Each bars represents mean ± SE (n=6) bearing different superscripts vary significantly (p <0.05) in Duncan's multiple comparison post-hoc test. [CON: Control, SA: Sodium arsenite, SM: Silymarin, SA+ SM: Sodium arsenite + Silymarin].

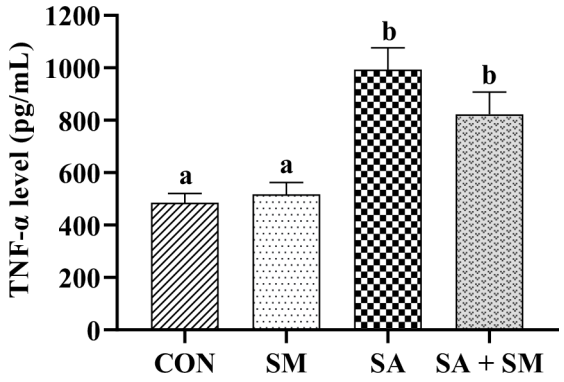


Figure 4: Effects of silymarin on tumour necrosis factor alpha (TNF-α) level (pg/mL) in the heart of sodium arsenite-exposed rats. Each bar represents the mean ± SE (n = 6) bearing different superscripts, which vary significantly (p <0.05) in Duncan's multiple comparison post-hoc test. [CON: Control, SA: Sodium arsenite, SM: Silymarin, SA+ SM: Sodium arsenite + Silymarin].

3.3.8 Creatine Kinase-Myocardial Bond (CK-MB)

Figure 3 showed the effect of SM on CK-MB level (IU/L) in SA-exposed rats. Control rats had a CK-MB level of 303.67 ± 51.50, and SM alone produced a marginal, non-significant increase (318.00 ± 38.36) in its level. In contrast, exposure to SA led to a sharp and statistically significant (p < 0.05) elevation in CK-MB, reaching 924.83 ± 59.16, while administration of SM significantly attenuated this elevation, reducing CK-MB to 475.00 ± 57.47 in SA-exposed rats, showing reversal of the toxic effect toward control levels

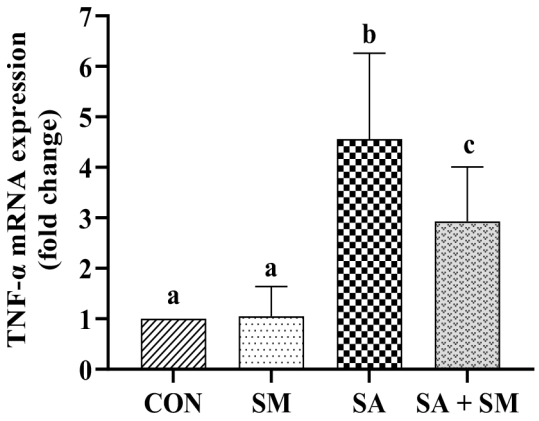


Figure 5: Effects of silymarin on mRNA expression of TNF-α in the heart of sodium arsenite-exposed rats. Each bars represents mean ± SE (n=6) bearing different superscripts vary significantly (p <0.05) in Duncan's multiple comparison post-hoc test. [CON: Control, SA: Sodium arsenite, SM: Silymarin, SA+ SM: Sodium arsenite + Silymarin].

3.3.9 Tumor Necrosis Factor-α (TNF-α) Assay

The effect of SM on TNF-α (pg/mL) levels in the heartsof SA-exposed rats was presented in Figure 4. Control rats showed TNF-α of 485.46 ± 34.78, and SM treatment alone (517.33 ± 44.74) showed similar values. Exposure to SA significantly (p < 0.05) elevated TNF-α to 993.20 ± 83.32, and subsequent SM treatment non-significantly reduced the levels to 822.96 ± 84.20, reflecting partial normalisation.

3.3.10 Quantitative RT-PCR:TNF-α mRNA Expression

The effect of SM on TNF-α mRNA expression (fold change) in the hearts of SA-exposed rats was shown in Figure 5. Control rats exhibited TNF-α mRNA expression of 1.00 ± 0.00, and this expression remained nearly unchanged following treatment with SM alone (1.05 ± 0.59) . SA exposure significantly (p < 0.05) upregulated TNF-α mRNA expression to (4.56 ± 1.70) fold. Treatment with SM in SA-exposed rats partially mitigated this elevation, lowering the expression to (2.91 ± 1.08) fold and suggesting a partial restoration toward control values.

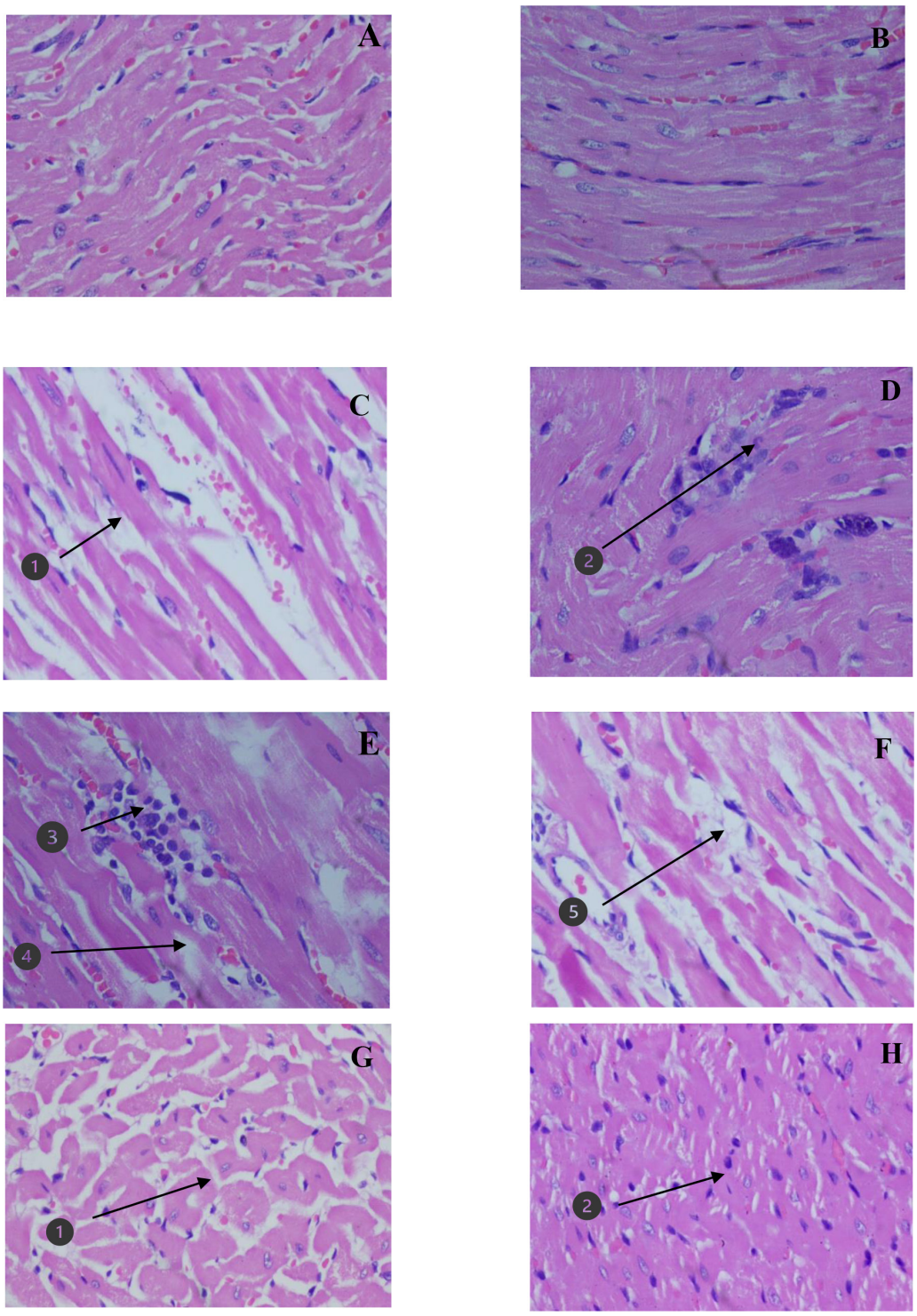


Figure 6: Histopathological examination of heart in H and E staining (40x) : Control group (**A**) and SM group (**B**) : normal architecture with endocardial layer contained collagen and elastic fibers beneath the endothelium, myocardium consisted of connective tissue with cardiac muscle fibers arranged in parallel and displaying clear striations. SA group (**C, D**) **:** haemorrhages with distorted myocardial cell and myofibres, disintegration of myocytes characterized by hyper eosinophilic cytoplasm, SA group (**E, F**) : myocyte shows loss of striation with focal myocardial necrosis, mononuclear cell infiltration and myocytic degeneration, fatty changes seen in myocyte. SA + SM group (**G, H**) : parallel orientation of myocytes along their nuclei, reduced necrosis and degeneration of cardiac fibres. [SA: Sodium arsenite, SM: Silymarin, SA + SM: Sodium arsenite + Silymarin].

3.4 Histopathological Evaluation of Heart Tissue

In the present study, the microscopic examination of heart sections from different experimental rat groups is illustrated in Figure 6. Histopathological analysis of the hearts from control and SM-treated rats revealed a normal architecture comprising three distinct layers *viz.* endocardium, myocardium, and epicardium. The endocardial layer contained collagen and elastic fibers beneath the endothelium, while the myocardium consisted of connective tissue with cardiac muscle fibers arranged in parallel and displaying clear striations (Figures 6a and 6b).

Figures 6c, 6d, 6e, 6f represented the sections of heart belonging to SA exposed rats showed haemorrhages with distorted myocardial cell, hemorrhages with myofibres distortion[1], multiple areas in the myocardial sections showed disintegration of myocytes characterized by hyper eosinophilic cytoplasm[2], certain myocyte shows loss of striation with focal myocardial necrosis[3] with mononuclear cell infiltration and myocytic degeneration[4] and fatty changes seen in myocyte[5].

Meanwhile, administration of SM in SA exposed rats showed parallel orientation of myocytes along their nuclei[1], reduced necrosis and degeneration of cardiac fibres[2] (Figures 6g and 6h) .

4. Discussion

The present study demonstrated that subacute exposure to SA induces marked cardiotoxicity characterized by metabolic stress, oxidative imbalance, inflammation, and structural myocardial injury. The clinical manifestations observed in SA-treated rats-including reduced feed intake, dehydration, and progressive loss of body weight-suggested impairment of mitochondrial function, compromised ATP generation, and gastrointestinal irritation, consistent with earlier findings by Ganie *et al.*, [27] and Wu *et al.*, [28]. These systemic alterations indicate early metabolic burden on cardiac tissue and contribute to the functional decline noted in the present study. Administration of SM effectively ameliorated these effects, as evidenced by improved feed intake and restoration of body condition. Such recovery is attributable to SM's mitochondrial-stabilising, antioxidant, and membrane-protective properties, which enhance metabolic resilience under toxic stress[29, 30].

SA exposure caused clear hematological disturbances that can aggravate cardiac stress by reducing oxygen delivery. The significant decreases in RBC count, haemoglobin, MCH, MCHC, and platelet numbers-while WBC and PCV remained unchanged-reflect arsenic's binding to haemoglobin sulfhydryl groups and its oxidative damage to erythrocyte membranes, leading to shortened RBC lifespan. SA also impaired erythropoiesis through GATA binding protein 1(GATA-1) downregulation, resulting in anemia and thrombocytopenia[31], consistent with findings from[32, 33]. SM treatment reversed these alterations, restoring RBC and Hb levels and improving MCH and platelet counts, in agreement with[29, 30]. These improvements reflect SM's antioxidant and membrane-protective actions that support erythrocyte stability and oxygen transport.

SA significantly increased CK-MB levels, confirming myocardial cell membrane damage. This elevation occurred because arsenic binds to sulfhydryl groups on sarcolemmal proteins and generates excess ROS, leading to loss of membrane integrity and leakage of cardiac enzymes-consistent with[34-36]. SM administration markedly reduced CK-MB, indicating protection of cardiomyocyte membranes. This effect aligns with[37, 30] and reflects SM's strong antioxidant and membrane-stabilizing properties that prevent oxidative disruption of myocardial cell membranes.

SA markedly elevated $O_2^{\bullet-}$levels in the heart, reflecting activation of mitochondrial ROS generation and NADPH oxidase pathways. These findings match earlier reports on arsenic-driven ROS overload and mitochondrial injury[36, 38]. Elevated LPO further indicates oxidative degradation of myocardial membranes. SM significantly reduced both $O_2^{\bullet-}$and LPO, consistent with its ability to inhibit NADPH oxidase and directly neutralize free radicals[17, 30]. Mechanistically, SM interrupts radical chain reactions and stabilizes membrane phospholipids, preventing myocardial oxidative injury.

SA drastically suppressed SOD, catalase, GPx, GR, and GSH levels, indicating collapse of the endogenous antioxidant defence system. Arsenic impairs these enzymes through direct binding to thiol groups, depletion of cofactors, and promotion of oxidative inactivation, as demonstrated in previous studies[33, 39, 40]. Depletion of GSH is particularly critical since GSH regulates detoxification and mitochondrial redox cycling. SM significantly restored these antioxidant systems, consistent with Sarfarpour *et al.*,[25] Salama *et al.*,[41] Okiljevic *et al.*,[16]. Mechanistically, SM

enhances GSH synthesis, stabilizes redox enzymes, and protects their active sites from oxidative inactivation.

SA significantly elevated TNF-α levels and mRNA expression, confirming activation of pro-inflammatory pathways. Arsenic induces TNF-α *via* nuclear factor kappa B (NF-κB) activation, mitochondrial swelling, and oxidative stress, leading to myocardial degeneration and fibrotic remodeling[42, 34]. SM markedly reduced TNF-α expression, consistent with findings of Safarpour *et al.*, [25] and Zheng *et al.*, [43]. Mechanistically, SM blocks NF-κB and Mitogen-Activated Protein Kinase (MAPK) signaling, preventing cytokine-driven myocardial injury.

SA produced severe myocardial lesions including haemorrhage, disrupted myofibrils, cytoplasmic eosinophilia, necrosis, inflammatory infiltration, and fatty degeneration. These lesions indicate structural collapse of cardiomyocytes and validate biochemical findings. Similar arsenic-associated cardiac pathology has been described by Oyagbemi *et al.*, [16] Goudarzi *et al.*, [32] Khuntia *et al.*, [35] SM treatment restored myocardial architecture, reducing necrosis and inflammation and preserving fiber orientation, consistent with protective effects described by Aktas *et al.*, [30] Jalil *et al.*,[37] and Mechanistically, SM stabilizes membranes, enhances mitochondrial integrity, and prevents inflammatory cell infiltration.

5. Conclusion

The present study conclusively establishes that SA exposure results in profound systemic and cardiac toxicity in male Wistar rats, characterized by reduced feed intake and body weight, perturbations in haematological and biochemical indices, amplified oxidative and nitrosative stress, increased inflammatory cytokines, and severe histopathological alterations in cardiac tissues. SM administration markedly alleviates these detrimental effects, contributing to improvements in physical, haematological, metabolic, antioxidant, and anti-inflammatory parameters, and preserving tissue integrity. Taken together, these findings demonstrate that SM exerts significant therapeutic effects against SA-induced cardiac injury in a preclinical rat model, although certain biochemical and histopathological alterations were not completely normalized, indicating partial recovery of cardiac tissue.

To advance this field, future investigations should focus on fine-tuning SM dosing strategies and exploring its performance in prolonged or recurrent SA exposure models. Further mechanistic investigations including apoptosis, mitochondrial stability, inflammatory signalling, pharmacokinetics, safety profiling, and functional cardiac evaluation are required before clinical applicability can be established.

6. Acknowledgements

The authors gratefully acknowledge the Karnataka Veterinary, Animal and Fishery Sciences University, Bidar for providing the necessary facilities to carry out this research study.

7. Reference

1. Jomova K, Jenisova Z, Feszterova M, Baros S, Liska J, Hudecova D, Rhodes CJ, Valko M. Arsenic: toxicity, oxidative stress and human disease. J Appl Toxicol. 2011; 31(2):95-107. https://doi.org/10.1002/jat.1649 PMid:21321970 PMCid:PMC10810663.
2. Argos M, Kalra T, Rathouz PJ, Chen Y, Pierce B, Parvez F, Islam T, Ahmed A, Rakibuz-Zaman M, Hasan R, Sarwar G, Slavkovich V, van Geen A, Graziano J, Ahsan H. Arsenic exposure from drinking water, and all-cause and chronic-disease mortalities in Bangladesh (HEALS): a prospective cohort study. Lancet. 2010; 376(9737):252-258. https://doi.org/10.1016/S0140-6736(10) 60481-3 PMid:20646756 PMCid:PMC3951449.
3. Chen Y, Graziano JH, Parvez F, Liu M, Slavkovich V, Kalra T, Argos M, Islam T, Ahmed A, Rakibuz-Zaman M, Hasan R, Sarwar G, Levy D, van Geen A, Ahsan H. Arsenic exposure from drinking water and mortality from cardiovascular disease in Bangladesh: prospective cohort study. BMJ. 2011; 342:2431. https://doi.org/10.1136/bmj.d2431 PMid:21546419 PMCid:PMC3088786.
4. WHO (World Health Organization) . 2011. Guideline for drinking-water quality, WHO Press, 20 Avenue Appia, Geneva 27., 38(4):104-108
5. Roy D, Kumar Das T, Vaswani S. Arsenic: its extent of pollution and toxicosis: An animal perspective. Veterinary World. 2013; 6(1). https://doi.org/10.5455/vetworld.2013.53-58
6. Stea F, Bianchi F, Cori L, Sicari R. Cardiovascular effects of arsenic: clinical and epidemiological findings. Environ Sci Pollut Res Int. 2014; 21(1):244-251. https://doi.org/10.1007/s11356-013-2113-z PMid:24019140.
7. Hu Y, Li J, Lou B, Wu R, Wang G, Lu C, Wang H, Pi J, Xu Y. The Role of Reactive Oxygen Species in Arsenic Toxicity. Biomolecules. 2020; 10(2):240. https://doi.org/10.3390/biom10020240 PMid:32033297 PMCid:PMC7072296.

8. Speer RM, Zhou X, Volk LB, Liu KJ, Hudson LG. Arsenic and cancer: Evidence and mechanisms. Adv Pharmacol. 2023; 96:151-202. https://doi.org/10.1016/bs.apha.2022.08.001 PMid:36858772 PMCid:PMC10860672.
9. Oyagbemi AA, Omobowale TO, Asenuga ER, Ochigbo GO, Adejumobi AO, Adedapo AA, Yakubu MA. Sodium arsenite-induced cardiovascular and renal dysfunction in rat via oxidative stress and protein kinase B (Akt/PKB) signaling pathway. Redox Rep. 2017; 22(6):467-477. https://doi.org/10.1080/13510002.2017.1308910 PMid:28366046 PMCid:PMC8900624.
10. Huang AL, Yang F, Cheng P, Liao DY, Zhou L, Ji XL, Peng DD, Zhang L, Cheng TT, Ma L, Xia XG. Honokiol attenuates the arsenic trioxide-induced cardiotoxicity by reducing the myocardial apoptosis. Pharmacol Res Perspect. 2022; 10(2):00914. https://doi.org/10.1002/prp2.914 PMid:35171536 PMCid:PMC8848632.
11. Pan X, Han H, Wang L, Yang L, Li R, Li Z, Liu J, Zhao Q, Qian M, Liu M, Du B. Nitidine Chloride inhibits breast cancer cells migration and invasion by suppressing c-Src/FAK associated signaling pathway. Cancer Lett. 2011; 313(2):181-191. https://doi.org/10.1016/j.canlet.2011.09.001 PMid:21959111.
12. Muthumani M, Prabu SM. Silibinin potentially attenuates arsenic-induced oxidative stress mediated cardiotoxicity and dyslipidemia in rats. Cardiovasc Toxicol. 2014; 14(1):83-97. https://doi.org/10.1007/s12012-013-9227-x PMid:24062023.
13. Taghiabadi E, Imenshahidi M, Abnous K, Mosafa F, Sankian M, Memar B, Karimi G. Protective Effect of Silymarin against Acrolein-Induced Cardiotoxicity in Mice. Evid Based Complement Alternat Med. 2012; 352091. https://doi.org/10.1155/2012/352091 PMid:23320028 PMCid:PMC3535759.
14. Fleming, T. 2000. PDR for Herbal Medicines. New Jersy Medical Economics Company., 1: 516-518.
15. Khazaei R, Seidavi A, Bouyeh M. A review on the mechanisms of the effect of silymarin in milk thistle (Silybum marianum) on some laboratory animals. Vet Med Sci.2022; 8(1):289-301. https://doi.org/10.1002/vms3.641 PMid:34599793 PMCid:PMC8788984.
16. Okiljević B, Martić N, Govedarica S, AndrejićVišnjić B, Bosanac M, Baljak J, Pavlić B, Milanović I, Rašković A. Cardioprotective and Hepatoprotective Potential of Silymarin in Paracetamol-Induced Oxidative Stress. Pharmaceutics. 2024; 16(4):520. https://doi.org/10.3390/pharmaceutics16040520 PMid:38675181 PMCid:PMC11055062.
17. Soria EA, Eynard AR, Bongiovanni GA. Cytoprotective effects of silymarin on epithelial cells against arsenic-induced apoptosis in contrast with quercetin cytotoxicity. Life Sci. 2010; 87(9-10):309-315. https://doi.org/10.1016/j.lfs.2010.07.007 PMid:20637780.
18. Wang HD, Pagano PJ, Du Y, Cayatte AJ, Quinn MT, Brecher P, Cohen RA. Superoxide anion from the adventitia of the rat thoracic aorta inactivates nitric oxide. Circ Res. 1998; 82(7):810-818. https://doi.org/10.1161/01.RES.82.7.810 PMid:9562441.
19. Paula FB, Gouvêa CM, Alfredo PP, Salgado I. Protective action of a hexane crude extract of Pterodonemarginatus fruits against oxidative and nitrosative stress induced by acute exercise in rats. BMC Complement Altern Med. 2005; 5:17. https://doi.org/10.1186/1472-6882-5-17 PMid:16107219 PMCid:PMC1192789.
20. Madesh M, Balasubramanian KA. Microtiter plate assay for superoxide dismutase using MTT reduction by superoxide. Indian J BiochemBiophys. 1998; 35(3):184-188. PMID: 9803669.
21. Aebi, H, E. 1983. Catalase. In: Method of Enzymatic Analysis, VCH, Weinheim. Germany Deerfield, 3(1):273-286.
22. Paglia DE, Valentine WN. Studies on the quantitative and qualitative characterization of erythrocyte glutathione peroxidase. J Lab Clin Med. 1967; 70(1):158-69. PMID: 6066618.
23. Goldberg, D, M. and Spooner, R, J. 1983. Method of enzymatic analysis. Glutathione reductase. Volume 3. Edn 3rd. Weinhein, Deerfield Beach., 258-265.
24. Sedlak J, Lindsay RH. Estimation of total, protein-bound, and nonprotein sulfhydryl groups in tissue with Ellman's reagent. Anal Biochem. 1968; 25(1):192-205. https://doi.org/10.1016/0003-2697(68) 90092-4 PMid:4973948.
25. Safarpour S, Safarpour S, Moghadamnia AA, Kazemi S, Ebrahimpour A, Shirafkan F, Mansoori R, Golchoobian R. Cardioprotective effect of silymarin nanoemulsion on 5-fluorouracil-induced cardiotoxicity in rats. Arch Pharm (Weinheim) . 2022; 355(7):2200060. https://doi.org/10.1002/ardp.202200060 PMid:35411625.
26. Livak KJ, Schmittgen TD. Analysis of relative gene expression data using real-time quantitative PCR and the 2(-Delta Delta C(T)) Method. Methods. 2001; 25(4):402-408. https://doi.org/10.1006/meth.2001.1262 PMid:11846609.
27. Ganie SY, Javaid D, Hajam YA, Reshi MS. Arsenic toxicity: sources, pathophysiology and mechanism. Toxicol Res (Camb) . 2023; 13(1):111. https://doi.org/10.1093/toxres/tfad111 PMid:38178998 PMCid:PMC10762673.
28. Wu J, Wen L, Liu X, Li Q, Sun Z, Liang C, Xie F, Li X. Silybin: A Review of Its Targeted and Novel Agents for Treating Liver Diseases Based on Pathogenesis. Phytother Res. 2024; 38(12):5713-5740. https://doi.org/10.1002/ptr.8347 PMid:39310970.
29. Dangleben NL, Skibola CF, Smith MT. Arsenic immunotoxicity: a review. Environ Health. 2013; 12(1):73. https://doi.org/10.1186/1476-069X-12-73 PMid:24004508 PMCid:PMC3848751.

30. Aktas, I. and Ozgocmen, M. The treatment effect of silymarin on heart damage in rats. Ann. Med. Res. 2020; 27(3):948-954. https://doi.org/10.5455/annalsmedres.2019.10.643
31. Zhou X, Medina S, Bolt AM, Zhang H, Wan G, Xu H, Lauer FT, Wang SC, Burchiel SW, Liu KJ. Inhibition of red blood cell development by arsenic-induced disruption of GATA-1. Sci Rep. 2020; 10(1):19055. https://doi.org/10.1038/s41598-020-76118-x PMid:33149232 PMCid:PMC7643154.
32. Goudarzi M, Fatemi I, Siahpoosh A, Sezavar SH, Mansouri E, Mehrzadi S. Protective Effect of Ellagic Acid Against Sodium Arsenite-Induced Cardio- and Hematotoxicity in Rats. Cardiovasc Toxicol. 2018; 18(4):337-345. https://doi.org/10.1007/s12012-018-9446-2 PMid:29383632.
33. Hosseinzadeh A, Houshmand G, Goudarzi M, Sezavar SH, Mehrzadi S, Mansouri E, Kalantar M. Ameliorative effect of gallic acid on sodium arsenite-induced spleno-, cardio- and hemato-toxicity in rats. Life Sci. 2019; 217:91-100. https://doi.org/10.1016/j.lfs.2018.11.050 PMid:30472295.
34. Albtoosh A, Karawya F, Al-Naymat W, Al-Qaitat A. Potential Protective Effect of Spirulina Platensis on Sodium Arsenite Induced Cardiotoxicity in Male Rats. Tissue Barriers. 2022; 10(2):1983330. https://doi.org/10.1080/21688370.2021.1983330 PMid:34615441 PMCid:PMC9067523.
35. Khuntia G, Dash JR, Jena B, Mishra UK, Parija SC. Hesperidin attenuates arsenic trioxide-induced cardiac toxicity in rats. Asian Pacific Journal of Tropical Biomedicine. 2023; 13(4):156-164. https://doi.org/10.4103/2221-1691.374232
36. Thangapandiyan S, Hema T, Miltonprabu S, Paulpandi M, Dutta U. Sulforaphane ameliorate Arsenic induced cardiotoxicity in rats: Role of PI3k/Akt mediated Nrf2 signaling pathway. J Biochem Mol Toxicol. 2024; 38(1):23576. https://doi.org/10.1002/jbt.23576 PMid:37906532.
37. Jalil DM, Altaei T. Efficacy and Bioavailability of Silymarin on Plasma S100B Level in Cardiotoxicity-induced Rats. Biomed Pharmacol J. 2024; 17(1):565-578. https://doi.org/10.13005/bpj/2883
38. Han X, Yang Y, Zhang M, Chu X, Zheng B, Liu C, Xue Y, Guan S, Sun S, Jia Q. Protective Effects of 6-Gingerol on Cardiotoxicity Induced by Arsenic Trioxide Through AMPK/SIRT1/PGC-1α Signaling Pathway. Front Pharmacol. 2022; 13:868393. https://doi.org/10.3389/fphar.2022.868393 PMid:35571130 PMCid:PMC9096219.
39. Sun X, Wang X, He Q, Zhang M, Chu L, Zhao Y, Wu Y, Zhang J, Han X, Chu X, Wu Z, Guan S. Investigation of the ameliorative effects of baicalin against arsenic trioxide-induced cardiac toxicity in mice. Int Immunopharmacol. 2021; 99:108024. https://doi.org/10.1016/j.intimp.2021.108024 PMid:34333357.
40. Panneerselvam L, Raghunath A, Ravi MS, Vetrivel A, Subramaniam V, Sundarraj K, Perumal E. Ferulic acid attenuates arsenic-induced cardiotoxicity in rats. Biotechnol Appl Biochem. 2020; 67(2):186-195. https://doi.org/10.1002/bab.1830 PMid:31584213.
41. Salama RM, Tayel SG. Silymarin attenuates escitalopram (cipralex) induced pancreatic injury in adult male albino rats: a biochemical, histological, and immunohistochemical approach. Anat Cell Biol. 2023; 56(1):122-136. https://doi.org/10.5115/acb.22.204 PMid:36624692 PMCid:PMC9989791.
42. Wang L, Shi W, Gao X, SreeHarsha N, Zhang D. Cardioprotective role of metformin against sodium arsenite-induced oxidative stress, inflammation, and apoptosis. IUBMB Life. 2020; 72(4):749-757. https://doi.org/10.1002/iub.2174 PMid:31587475.
43. Zheng Y, Chen J, Wu X, Zhang X, Hu C, Kang Y, Lin J, Li J, Huang Y, Zhang X, Li C. Enhanced anti-inflammatory effects of silibinin and capsaicin combination in lipopolysaccharide-induced RAW264. 7 cells by inhibiting NF-κB and MAPK activation. Front. Chem. 2022; 10:934541. https://doi.org/10.3389/fchem.2022.934541 PMid:35844639 PMCid:PMC9279934.

Access this journal online	
Website: https://informaticsjournals.com/journals/toxi/home	**Quick Response Code**